ORGANOMETALLICS

Article

pubs.acs.org/Organometallics

Carbostannolysis Mediated by Bis(pentamethylcyclopentadienyl)lanthanide Catalysts. Utility in Accessing Organotin Synthons

Stephen D. Wobser, Casey J. Stephenson, Massimiliano Delferro,* and Tobin J. Marks*

Department of Chemistry, Northwestern University, Evanston, Illinois 60208-3113, United States

Supporting Information

ABSTRACT: Facile carbon−tin bond activation in the reaction of 2-(trimethylstannyl)pyridine (**1**) with the organolanthanide complexes $Cp^*_2LaCH(TMS)_2$ (**2a**) and $[Cp^*_2LaH]_2$ (**2b**) yields $Cp^*_2La(2\text{-pyridyl})$ (**3**), as well as $Me_3SnCH(TMS)_2$ and Me_3SnH, respectively. At room temperature, ethylene then undergoes insertion into the resulting La−C(pyridyl) bond followed by carbostannolysis to catalytically generate 2-(2-(Me_3Sn)ethyl)-pyridine (**4**) or, with extended reaction times, 6-ethyl-2-(2-(trimethylstannyl)ethyl)pyridine (**5**). In contrast to **1**, 6-methyl-2-(trimethylstannyl)pyridine (**6**) is unreactive, likely reflecting steric constraints. With terminal alkynes, this catalytic heterocycle−$SnMe_3$ activation/carbostannylation process affords tin-functionalized conjugated enynes. Thus, at 60 °C **2b** catalyzes the conversion **1** + 1-hexyne to yield (*E*)-2-butyl-1-(Me_3Sn)-oct-1-en-3-yne in a 60:1 ratio *E*:*Z* isomer ratio. This reaction is available to *α*-monosubstituted and *α*-disubstituted terminal alkynes, while *α*-trisubstituted alkynes are too hindered for reaction. The catalytic cycle is proposed to proceed via a spectroscopically detectable Me_3Sn−alkynyl intermediate which undergoes insertion into a Cp^*_2La−alkynyl bond to produce the conjugated alkynyl product, which is subsequently protonolyzed from the Cp^*_2La center by a new terminal alkyne substrate molecule. NMR spectroscopic and kinetic data support the proposed pathway and indicate turnover-limiting alkyne insertion.

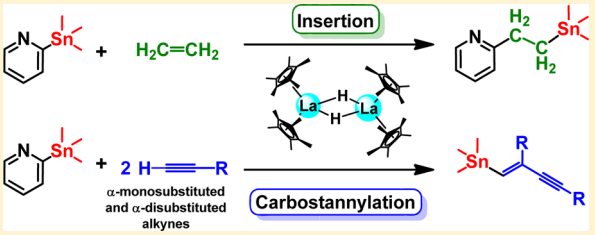

INTRODUCTION

Reagents having C−Sn linkages find widespread application in chemical synthesis.[1] For this reason, understanding and manipulating their reactivity with organometallic catalysts is of fundamental importance. Organotin reagents play an important synthetic role due to their selective reactivity, stability, and ease of handling.[2] There is also growing interest in using organotin reagents for transmetalation reactions[3] that traditionally employ toxic organomercury reagents.[4] In particular, the carbostannylation of alkynes, a process in which a Sn−C bond is added across a C≡C unsaturation (Scheme 1), is a powerful synthetic tool which simultaneously

Scheme 1. Generic Alkyne Carbostannylation Reaction

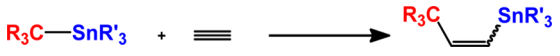

forms new C−C and C−Sn linkages.[5] The resulting Sn-functionalized alkenes can be readily employed as synthetic building blocks through Stille coupling reactions.[2c,6] Sn-functionalized enynes have particularly significant synthetic utility due to the adjacent conjugation,[5e,i,7] and such building blocks have demonstrated applications in arylation,[8] alkylation,[5b] and subsequent cyclization[9] reactions (e.g., Scheme 2). For example, facile Sn/Li transmetalation, followed by functionalization with an alcohol can be used to prepare a

Scheme 2. Representative Reactions of Tin-Functionalized Conjugated Enynes[5b]

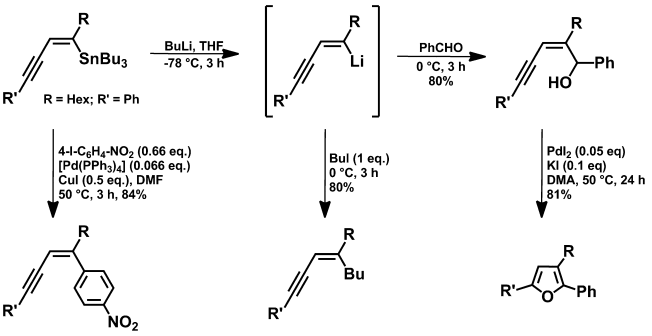

variety of enynols, which are readily cyclized to give functionalized furans. Furthermore, (*Z*)-enynols[10] have demonstrated pharmacological activity, including as potent antitumor agents.[11]

Catalytic carbostannylation is achieved using transition-metal agents such as palladium,[5d−g,i,j,7b] gold,[12] nickel,[5h] or ruthenium[5b] or by radical processes.[13] Frequently these

Special Issue: Recent Advances in Organo-f-Element Chemistry

Received: October 31, 2012

catalysts are limited to alkyne substrates having electron-withdrawing substituents, and for this reason there is a need for new approaches to the carbostannylation of unfunctionalized alkynes.

Additionally, in these reported transformations, the product alkene stereochemistry can be highly dependent on the nature of the substrate. Each of these metal-catalyzed processes involves oxidative addition/reductive elimination steps in the catalytic cycle. Lanthanide ions, on the other hand, typically have one readily accessible oxidation state and do not undergo traditional oxidative addition/reductive elimination sequences. Therefore, a lanthanide-catalyzed carbostannylation process would be expected to proceed through a very different mechanism. The utility of the product vinylstannanes and the limitations of the current synthetic methods provide an impetus to pursue alternative carbostannylation approaches, which is the topic of the present contribution.

Several heterocycle classes, including pyridines,[14] furans,[15] and thiophenes,[16] are known to undergo C−H activation at the 2-position by organolanthanide catalysts.[17] Although activation at the pyridine 2-position is most extensively documented, examples of subsequent catalytic alkylation are rare.[14a,i,l,18] This regioselectivity is thought to be directed by coordination of the strongly electrophilic lanthanide center to the heteroelement lone pair(s),[14c,d,f,i,j] thereby preorganizing the α-C−H bond proximate to the metal center and providing an intramolecular entropic advantage for C−H activation (e.g., Scheme 3).

Scheme 3. Activation of Pyridine at the 2-Position by an Organolanthanide Hydride

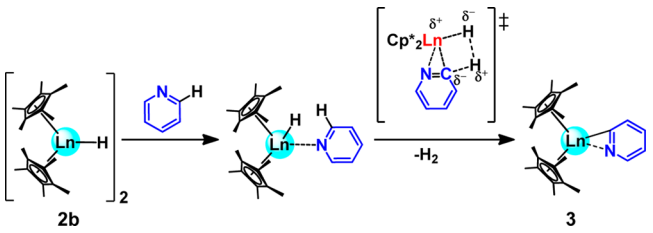

Cationic zirconocene catalysts also display similar α-activation selectivity with a variety of pyridine derivatives.[19] Note that this reactivity mode is operative for the insertion of various unsaturated groups into the pyridine α−C-H bond.[14a,b,i,20] For example, the reaction of ethylene with pyridine, catalyzed by $[Cp^*_2MH]_2$ (M = La[20] (**2b**), Y[14i]), produces 2-ethylpyridine, as shown in Scheme 4A. The selective insertion of a single ethylene molecule is attributed to the high stability of the five-membered ring formed upon chelation of the 2-(2-pyridyl)ethyl substituent (structure **7**, Scheme 4A).[14h,i] While similar organolanthanide activation of thiophene occurs via an analogous pathway, the reaction with ethylene yields distinctly different results. The chelating product formed after a single ethylene insertion is less tightly bound by the relatively less Lewis basic/softer thiophene substituent,[16,20] and multiple ethylene insertions are achieved using **2b** at elevated pressures, affording thiophene-capped polyethylenes (Scheme 4B).[16]

This reactivity of heterocyclic α-C−H positions with organolanthanides raises the intriguing question of whether similar processes might be employed to activate other heterocyclic 2-position functionalities such as organometalloids. For example, trialkyltin groups might be catalytically transferred from the heterocyclic 2-position to generate valuable new organotin compounds. If α-C−SnR_3 activation using 2-(trimethylstannyl)pyridine (**1**) as the substrate proceeded similarly, subsequent insertive chemistry at Cp^*_2La(2-pyridyl) (**3**) would then produce Cp^*_2La(2-(2-pyridyl)ethyl) complexes. Subsequent α-C−SnR_3/C−La σ-bond metathesis by a new molecule of **1** would then regenerate **3** and produce 2-[2-(trimethylstannyl)ethyl]pyridine (**4**). In this study we explore the novel activation of 2-(Me_3Sn)arenes as an approach to accessing a variety of novel organotin species. It will be seen that ethylene undergoes insertion into the La−C bond of the Cp^*_2La(2-pyridyl) (**3**) intermediate at 25 °C, followed by carbostannolysis, to catalytically generate 2-(2-(trimethylstannyl)ethyl)pyridine (**4**). Furthermore, the organolanthanide alkyl $Cp^*_2LaCH(TMS)_2$ (**2a**) and organolanthanide hydride $(Cp^*_2LaH)_2$ (**2b**) both initiate the conversion of 2-(trimethylstannyl)pyridine (**1**) with 1-hexyne to yield (*E*)-2-butyl-1-(trimethylstannyl)-oct-1-en-3-yne ((***E*****-9**). This transformation appears to be general for α-monosubstituted and α-disubstituted terminal alkynes.

Scheme 4. Catalytic Cycles Proposed by Teuben et al. for the Reaction of Ethylene and (A) Pyridine or (B)[a] Thiophene Mediated by Lanthanocene/Pseudolanthanocene Catalysts[14i,16,20]

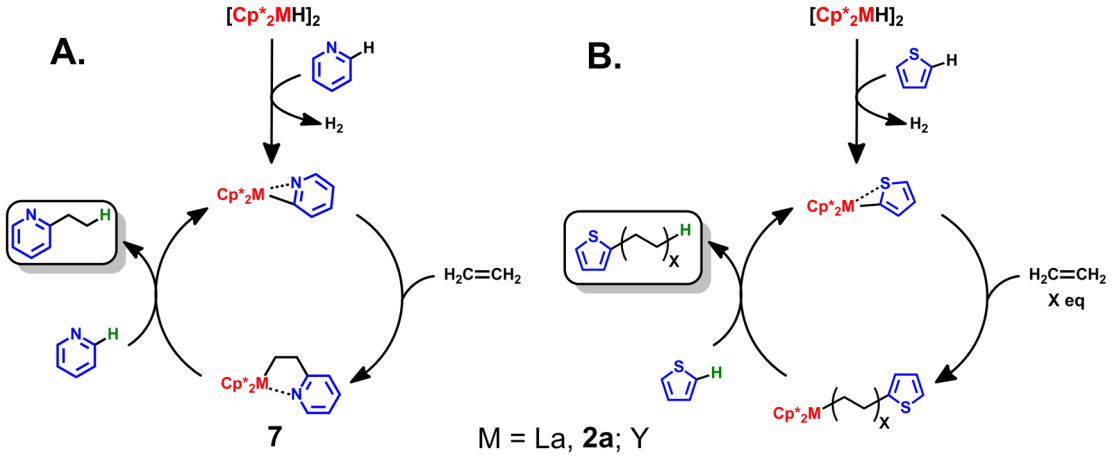

[a]Note that cycle B is extremely sluggish for M = Y.

dx.doi.org/10.1021/om301031e | *Organometallics* XXXX, XXX, XXX−XXX

EXPERIMENTAL SECTION

Materials and Methods. All manipulations of air-sensitive materials were carried out with rigorous exclusion of O_2 and moisture in flame- or oven-dried Schlenk-type glassware on either a dual-manifold Schlenk line, interfaced to a high-vacuum manifold (10^{-6} Torr), or in a N_2-filled MBraun glovebox with a high-capacity recirculator (<1 ppm O_2). Argon (Airgas) was purified by passage through a MnO column to remove O_2 and a column of Davison 4A molecular sieves to remove water immediately before use. Solvents for catalytic reactions were stored over Na/K alloy in resealable containers and vacuum-transferred immediately prior to use. All liquid or volatile solid substrates for catalytic experiments were dried over a series of three or more beds of freshly activated Davison 4Å molecular sieves as solutions in benzene-d_6 or toluene-d_8 (Cambridge Isotope Laboratories, 99+ atom % D). Substrate solutions were degassed by freeze–pump–thaw methods. Solid substrates were purified by sublimation under high vacuum and were stored at −35 °C in a glovebox. The NMR internal integration standard, trimethylphenylsilane, was sublimed and exposed to high vacuum overnight before storage in the glovebox. The precatalysts $Cp^*_2LaCH(TMS)_2$ (**2a**) and $(Cp^*_2LaH)_2$ (**2b**) were prepared as reported in the literature.[21] Substrates cyclohexylacetylene, 1-hexyne, and *tert*-butylacetylene were purchased from Sigma-Aldrich. Substrate **1** was purchased from TCI. The substrates 2-(trimethylstannyl)furan,[22] 2-(trimethylstannyl)-thiophene,[23] and 6-methyl-2-(trimethylstannyl)pyridine (**6**)[24] were prepared as reported in the literature, and spectra agree with literature values.

Physical and Analytical Measurements. NMR spectra were recorded on a Mercury 400 (400 MHz, ^{1}H; 100 MHz, ^{13}C; 149.1 MHz, ^{119}Sn), Inova 500 (500 MHz, ^{1}H; 125 MHz, ^{13}C), or Bruker Avance III 500 instrument (500 MHz, ^{1}H; 125, ^{13}C). Chemical shifts (δ) for ^{1}H and ^{13}C are referenced to internal solvent resonances and reported relative to $SiMe_4$. ^{119}Sn NMR chemical shifts are reported relative to $SnMe_4$. Quoted values of ^nJ(Sn−C) refer to ^nJ(^{119}Sn−C) when the ^{119}Sn and ^{117}Sn satellites are resolvable. NMR experiments on air-sensitive samples were conducted in Teflon-valve-sealed J. Young NMR tubes. High-resolution mass spectra were acquired on a Waters GC-TOF GCT Premier Micromass MS.

NMR-Scale Reaction of 2-(Trimethylstannyl)pyridine (1) with Ethylene. In the glovebox, 8.4 mg (0.015 mmol) of **2a** was weighed into a vial, dissolved in 0.5 mL of toluene-d_8, and transferred by pipet to a J. Young NMR tube. The sealed tube was removed from the glovebox and then interfaced to a high-vacuum manifold, and 0.2 mL of a 1.0 M solution of **1** (0.2 mmol) was added. The tube was degassed by manual agitation and brief exposure to vacuum and then cooled to −78 °C and exposed to 1.0 atm of ethylene. The tube was then warmed to room temperature and shaken, and the ensuing reaction was monitored by NMR. Since most ethylene was consumed within 90 min at room temperature, this procedure for adding ethylene was repeated. After 16 h at room temperature, reaction progress had plateaued, and no further consumption of ethylene was observable over an additional 2 days at room temperature. The product, 6-ethyl-2-(2-trimethyltin)ethylpyridine (**5**), was characterized by ^{1}H, ^{13}C, COSY, and HSQC NMR (see the Supporting Information). HMBC NMR confirms that both ethyl groups are bound to the 2- and 6-positions of a single pyridine core.

Preparative-Scale Reaction of 2-(Trimethylstannyl)pyridine (1) with Ethylene. In the glovebox, a three-neck Morton flask was charged with 25 mL of dry toluene and 12.0 mg (0.020 mmol) of **2b**. The apparatus was removed from the glovebox and interfaced to a high-vacuum manifold. To this solution was added 1.0 mL of a 1.0 M solution of **1** in toluene (1.0 mmol) by syringe under argon flush. The solution was stirred and degassed by brief exposure to high vacuum. After 15 min, the degassed solution was exposed to a feed of 1.0 atm of ethylene for 2.0 h with vigorous stirring. The reaction was quenched with 10 mL of methanol, and the volatiles were removed under vacuum, leaving a colorless oil. The oil was determined by ^{1}H NMR and GC/MS to be an ∼83:2:15 ratio mixture of 2-[2-(trimethylstannyl)ethyl]pyridine (**4**) to 6-ethyl-2-[2-(trimethylstannyl)ethyl]pyridine (**5**) to starting material **1** with ∼5% unidentified impurities in the ^{1}H NMR, which were undetectable by GC/MS.

Preparative-Scale Reaction of 6-Methyl-2-(trimethylstannyl)pyridine (6) with Ethylene. This reaction was carried out by following the procedure for the reaction of 2-(trimethylstannyl)pyridine with ethylene described above. Only starting material was recovered from the reaction vessel.

Catalytic Carbostannylation of Alkynes with 2-(Trimethylstannyl)pyridine (1). In a glovebox, a J. Young NMR tube was charged with a weighed amount of the precatalyst **2b** (ca. 4.1 mg, 0.010 mmol) and the internal standard Ph_3SiMe (ca. 50 μmol, 13.5 mg). The tube was then interfaced to a high-vacuum line and substrate solutions of the alkyne (ca. 0.20 mL of a 1.0 M solution in C_6D_6, 0.20 mmol) and 2-(trimethylstannyl)pyridine (**1**; ca. 0.48 mL, 1.0 M solution in C_7D_8, 0.48 mmol) were added via syringe to a manifold chamber directly above the NMR tube. The solutions were mixed immediately before addition to the NMR tube at −78 °C. After the NMR tubes were sealed, the reaction mixtures were warmed to room temperature and shaken vigorously. Each reaction tube was then placed in a preheated NMR spectrometer (±0.2 °C, verified by an ethylene glycol standard) and allowed to equilibrate for at least 6 min before data collection began. Data were obtained with a single transient to avoid signal saturation. Heating subsequent to the initial 12 h was carried out in temperature-controlled oil baths, from which reaction mixtures were periodically removed for NMR analysis. Substrate and/or product concentrations were determined relative to the intensity of the internal standard resonance plotted versus time. Upon completion, the reaction mixtures were filtered through a plug of basic alumina to separate the products, and volatiles were removed in vacuo.

Kinetic Analysis. Kinetic analysis of the NMR-scale reactions described above was carried out by collecting numerous (>15) data points early in the reaction before substrate concentrations were appreciably depleted.[25] Under these conditions, the reaction can be approximated as pseudo zero order with respect to the substrate concentrations. Data were fit by least-squares analysis ($R^2 > 0.995$) according to eq 1, where t is time and [product] is the concentration of product at time t. The turnover frequency (N_t) was then calculated according to eq 2, where $[\text{catalyst}]_0$ is the initial catalyst concentration.

$$[\text{product}] = mt \tag{1}$$

$$N_t\ (\text{h}^{-1}) = \frac{m}{[\text{catalyst}]_0} \tag{2}$$

(*Z*)-2,4-Dicyclohexyl-1-(trimethylstannyl)-but-1-en-3-yne ((*Z*)-8). ^{1}H NMR (500 MHz, C_6D_6): δ 6.11 (s, 1H; 80.8 Hz, ^2J (^{119}Sn−^{1}H), 2.40 (t, 1H), 2.13 (t, 1H), 1.11−1.94 (m, 20H), 0.29 (s, 9H; 54.4, ^2J (^{119}Sn−^{1}H)). ^{13}C NMR (125 MHz, C_6D_6): δ 148.52, 133.44, 95.45, 83.09, 49.90, 33.73, 33.62, 33.19, 33.15, 33.08, 26.88, 25.85, −8.44 (354.4 Hz, ^2J (^{119}Sn−^{1}H)). ^{119}Sn NMR (149.1 MHz, C_6D_6): δ −52.49. MS (m/z): [(M − Me)$^+$] calcd for $C_{18}H_{29}Sn$, 365.129; found, 365.127.

(*Z*)-2-Butyl-1-(trimethylstannyl)-oct-1-en-3-yne ((*Z*)-9). ^{1}H NMR (500 MHz, C_6D_6): δ 6.12 (s, 1H; 82.2 Hz, ^2J (^{119}Sn−^{1}H), 2.31 (t, 2H), 2.16 (t, 2H), 1.61 (m, 2H), 1.40 (m, 2H), 1.34 (m, 2H), 1.31 (m, 2H), 0.88 (t, 3H), 0.80 (t, 3H), 0.31 (s, 9H). ^{13}C NMR (125 MHz, C_6D_6): δ 142.96, 136.26, 90.82, 83.87, 42.07, 31.54, 31.47, 22.87, 22.70, 19.69, 14.57, 14.08, −8.68 (354.9 Hz, ^2J (^{119}Sn−^{1}H)). ^{119}Sn NMR (149.1 MHz, C_6D_6): δ −53.66. MS (m/z): [(M −- Me)$^+$] calcd for $C_{14}H_{25}Sn$, 313.098; found, 313.315.

(*E*)-2-Butyl-1-(trimethylstannyl)-oct-1-en-3-yne ((*E*)-9). ^{1}H NMR (500 MHz, C_6D_6): δ 6.44 (s, 1H; 70.4 Hz, ^2J (^{119}Sn−^{1}H), 2.26 (t, 2H), 2.21 (t, 2H), 1.72 (m, 2H), 1.40 (m, 2H), 1.37 (m, 2H), 1.35 (m, 2H), 0.91 (t, 3H), 0.81 (t, 3H), 0.14 (s, 9H). ^{13}C NMR (125 MHz, C_6D_6): δ 141.95, 137.10, 89.12, 83.65, 40.50, 32.34, 31.76, 23.18, 22.63, 19.71, 14.71, 14.11, −8.31 (352.6 Hz, ^2J (^{119}Sn−^{1}H)). ^{119}Sn NMR (149.1 MHz, C_6D_6): δ −55.45. MS (m/z): [(M − Me)$^+$] calcd for $C_{14}H_{25}Sn$, 313.098; found, 312.850.

dx.doi.org/10.1021/om301031e | *Organometallics* XXXX, XXX, XXX–XXX

RESULTS

The goal of this research was to investigate the activation of the Sn−C(aryl) bond in 2-(trimethylstannyl)pyridine (**1**) by the organolanthanide complexes/precatalysts $Cp^*_2LaCH(TMS)_2$ (**2a**) and $[Cp^*_2LaH]_2$ (**2b**) in the presence of C−C unsaturation. The reaction of **2a** with **1** is found to be significantly slower than that of complex **2b**, likely due to the steric congestion around the metal center. For ethylene, the reaction proceeds through a Cp^*_2La(2-pyridyl) (**3**) intermediate identified by NMR spectroscopy, followed by C=C insertion into the resulting La−C bond and subsequent carbostannolysis to generate 2-[2-(trimethylstannyl)ethyl]-pyridine (**4**) catalytically. With terminal alkynes such as 1-hexyne, this (heterocycle)C−$SnMe_3$ activation/carbostannylation process yields Me_3Sn-functionalized conjugated enynes (*E*)-2-butyl-1-(trimethylstannyl)-oct-1-en-3-yne ((***E***)-**9**) in a 60:1 *E*:*Z* isomer ratio. This reaction is available to α-monosubstituted and α-disubstituted terminal alkynes, while α-trisubstitued alkynes are unreactive.

Ethylene Insertion Reactivity. Initial NMR-scale studies of the reaction of **1** with ethylene, catalyzed by **2a**, indicate that both the pyridine 2- and 6-positions can be activated by the metal center (Scheme 5). While organolanthanide-mediated

Scheme 5. Reaction of Pyridine Derivative 1 with Ethylene, Catalyzed by $Cp^*_2LaCH(TMS)_2$

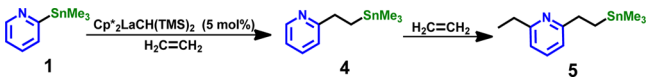

C−H bond activation at this position is established,[14a−k] C−Sn bond activation in this manner by d^0 or f^0 centers was previously unknown. In situ monitoring of the NMR-scale reaction indicates that the (pyridine)C−Sn bond is indeed activated and subsequent ethylene insertion occurs at this position (Scheme 5). Within 16 h at room temperature, the reaction is complete by NMR. The absence of characteristic ^{1}H NMR downfield pyridine signals at δ ∼8.5 indicates that the C−H α to the N atom has been selectively functionalized, and disappearance of the ^{117,119}Sn-coupled methyl signal at δ 0.32 indicates that the Me_3Sn group has been displaced. Furthermore, HSQC, COSY, and HMBC NMR spectra (see the Supporting Information) indicate there is a single pyridine skeleton in the product, substituted at both the 2- and 6-positions.

In situ ^{1}H NMR monitoring indicates that **4** is the predominant intermediate in the **1** → **5** conversion (Scheme 5). On the basis of these results, the reaction was next performed on a larger scale with excess ethylene in a stirred reactor. Note that these conditions do not effect the insertion of multiple ethylene units at either carbon position. However, insertion of a single ethylene into the C−Sn bond versus the α-C−H bond is observed with a selectivity of >100×, producing compound **4**. Halting the reaction with ∼85% of **1** consumed reveals minimal involvement of the α-C−H bond at this stage. The reaction can be quenched at this point or allowed to proceed through cycle B, where subsequent C−H activation/ethylene insertion yields **7**. Scheme 6 details a possible catalytic cycle for these transformations.

To investigate substrate steric effects, a preparative-scale reaction was carried out using 6-methyl-2-(trimethylstannyl)-pyridine (**6**) as the substrate. Here, ethylene insertion is not observed at either the 2- or the 6-position, and only starting material is recovered (eq 3).

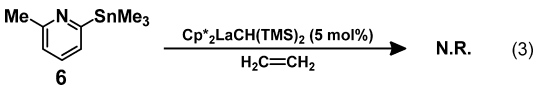

(3)

Reactivity of Terminal Alkynes. When hydride **2b** is treated with 20 equiv of substrate **1** and 48 equiv of cyclohexylacetylene at 60 °C for 12 h, followed by 120 °C overnight, both starting materials are completely consumed. Initial in situ ^{1}H NMR monitoring indicates essentially instantaneous H_2 formation (δ 4.48). After heating, ^{1}H, ^{13}C, HSQC, and HMBC NMR spectra of the reaction mixture (Supporting Information) indicate that the major products are (*Z*)-2,4-dicyclohexyl-1-(Me_3Sn)-but-1-en-3-yne, (***Z***)-**8**, and 1.0 equiv of pyridine (eq 4) with the double-bond *Z* orientation

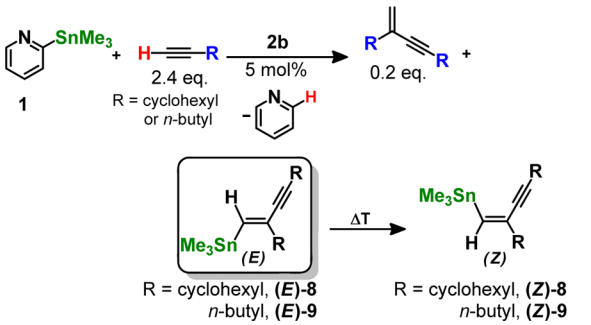

(4)

Scheme 6. Proposed Pathway for Conversion of Pyridine Derivative 1 to 4 and Then to 5

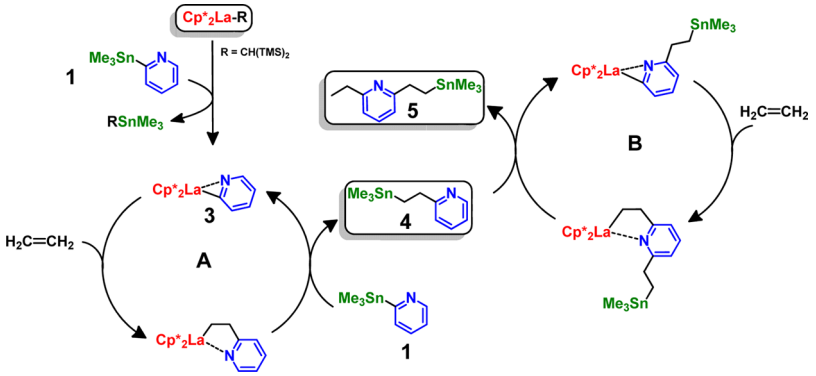

dx.doi.org/10.1021/om301031e | *Organometallics* XXXX, XXX, XXX−XXX

confirmed by NOESY NMR. Note that this stereochemistry determination was made *after heating at 120 °C overnight*. Furthermore, the excess cyclohexylacetylene is converted to an unfunctionalized dimer (eq 4) via a known organolanthanide-catalyzed process.[14h,26] When the above terminal alkyne + **1** reaction is repeated with 1-hexyne, the reaction is >90% complete within 1 day at only 60 °C by ^{1}H NMR (see Table 1).

Table 1. Alkyne Effects in Reactions with 2-(Trimethylstannyl)pyridine (1) Catalyzed by 5 mol % $[Cp^*_2LaH]_2$

Alkyne	Product	Conversion[a] (%)	*E*:*Z* ratio[a]	Initial rate[b] (N_t, h^{-1})
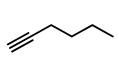	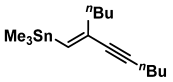	76	60. : 1	2.1
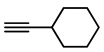	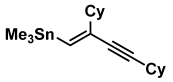	40	20. : 1	0.38
	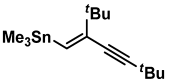	--	--	0.0

[a]At t = 12 h, by in situ ^{1}H NMR. [b]Initial rate derived from a linear fit (R^2 > 0.995) of product formation vs time for the first 5−15% conversion (see the Experimental Section for details).

Furthermore, NOESY NMR indicates that the product, (*E*)-**9**, has a double-bond orientation opposite to that of the cyclohexylacetylene product (*Z*)-**8**. Subsequent heating of (*E*)-**9** at 120 °C affords a mixture of (*E*)-**9** and (*Z*)-**9**. Clearly, the *E* isomer is the kinetic product and subsequently isomerizes to the *Z* product by known processes (vide infra). After 2.5 h of heating at 120 °C, nearly equivalent amounts of (*E*)-**9** and (*Z*)-**9** are present in the reaction mixture. Although the four *n*-butyl groups in the mixture overlap significantly in the ^{1}H NMR spectrum, several nonoverlapping, highly characteristic signals (i.e., vinyl, $SnMe_3$) are evident as well-separated signal pairs. Selective 1-D NOESY NMR irradiation of the (*Z*)-**9** $SnMe_3$ signal in the mixture confirms the stereochemistry (Figure 1). The ^{1}H NMR alkyl region shows a complex pattern from the four *n*-butyl groups in the isomeric mixture. However, HMBC and HSQC NMR spectroscopy allow unambiguous assignment of the ^{1}H and ^{13}C signals (Supporting Information). Elucidating the C═C orientation and subsequent isomerization process for product **9** prompted closer examination of the process forming (*Z*)-**8**. When the cyclohexylacetylene + **1** reaction is examined in situ by ^{1}H NMR, the *E*:*Z* isomer ratio is 95:5 after heating for 12 h at 60 °C. However, after heating overnight at 120 °C, the *E*:*Z* ratio falls to 11:89, arguing that the catalytic cycle first produces *E* C═C stereochemistry, which then undergoes isomerization by a known thermal/radical process (vide infra).[13,27] The reaction of **1** + cyclohexylacetylene without an organolanthanide catalyst was also investigated under identical conditions. After heating at 60 °C for 30 h, negligible reaction is observed by ^{1}H NMR, confirming that these processes are mediated by the organolanthanide catalyst.

Reaction Kinetics. The reaction of **1** with 1-hexyne catalyzed by **2b** was monitored in situ by NMR at 60 °C. The tin-coupled vinyl signal characteristic of product (*E*)-**9** was monitored, and conversion is plotted versus time in Figure 2. Note that the rate of product formation falls as the reaction proceeds. Note also that a number of new signals are observed in ^{1}H and ^{13}C NMR spectra of the 25 °C reaction mixture, corresponding to pyridine and the known compound Me_3Sn(1-hexynyl)[28] *before* any (*E*)-**9** is observed (Figure 3).

The proposed catalytic cycle in Scheme 7 accounts for the formation of the initially formed products (*E*)-**8** and (*E*)-**9**. Here, lanthanide hydride precatalyst **2b** is activated by the terminal alkyne substrate, generating Cp^*_2La−alkynyl species ***A*** and H_2, the latter of which is observed by ^{1}H NMR (δ 4.48). Cycle A in Scheme 7 may operate independently of cycle B and proceeds by a σ-bond metathesis with **1**, eliminating intermediate Me_3Sn(alkynyl) species ***B*** and generating

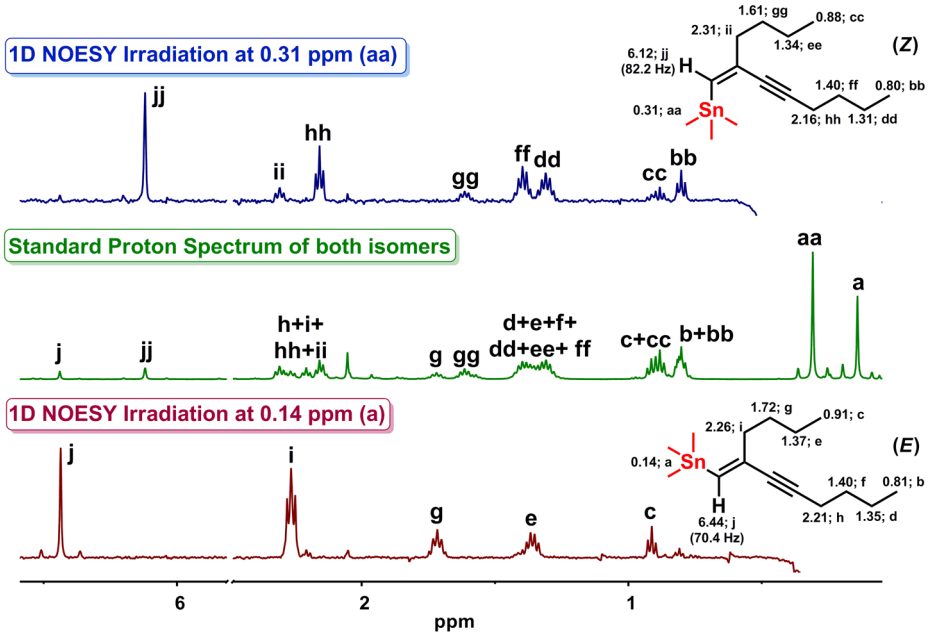

Figure 1. (middle) ^{1}H NMR of (*E*)-**9** and (*Z*)-**9** mixture from the **1** + 1-hexyne reaction (Scheme 8). (top) Selective irradiation of the $SnMe_3$ signal of (*Z*)-**9** using 1D NOESY NMR. (bottom) Selective irradiation of $SnMe_3$ of (*E*)-**9** using 1D NOESY NMR.

dx.doi.org/10.1021/om301031e | *Organometallics* XXXX, XXX, XXX−XXX

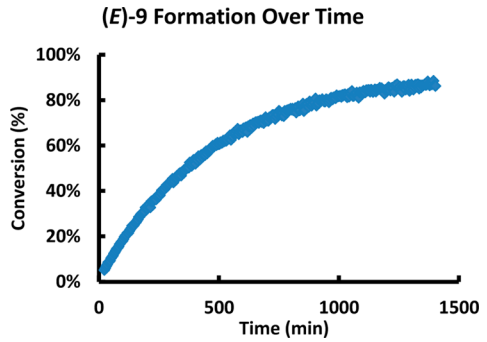

Figure 2. Plot of (*E*)-**9** formation versus time in the reaction of **1** + 1-hexyne catalyzed by organolanthanide complex **2b** (5 mol %) at 60 °C: $[\mathbf{1}]_0$ = 294 mM; $[\text{1-hexyne}]_0$ = 706 mM; $[\mathbf{2b}]_0$ = 14.7 mM.

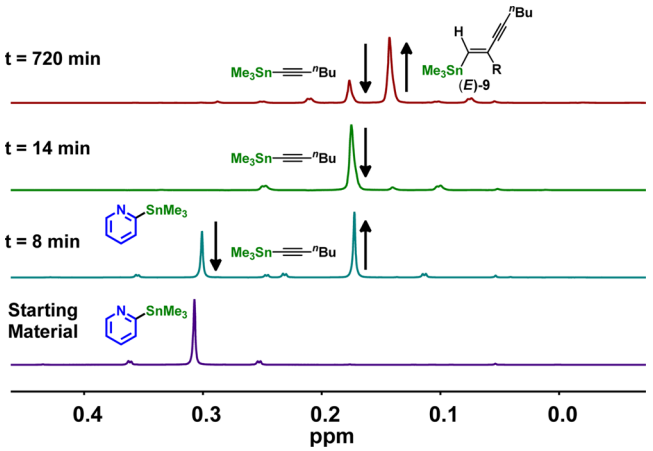

Figure 3. Stack plot showing the Me_3Sn region of the ^1H NMR spectra of the reaction of **1** with 1-hexyne catalyzed by **2b** (5 mol %): $[\mathbf{1}]_0$ = 294 mM; $[\text{1-hexyne}]_0$ = 706 mM; $[\mathbf{2b}]_0$ = 14.7 mM; *t* = 8 min, 25 °C; *t* = 14 min, 60 °C; *t* = 720 min, 60 °C.

Cp^*_2La-pyridyl complex **3** (cycle A, step *ii*). Species **3** then undergoes protonolysis by a new terminal alkyne substrate molecule (cycle A, step *iii*), eliminating pyridine and regenerating Cp^*_2La–alkynyl species ***A***. Cycle B then proceeds via insertion of intermediate ***B*** (generated from cycle A) into the La–alkynyl bond of ***A*** (cycle B, step *ii*). The resulting Cp^*_2La–vinyl complex ***C*** produced in this reaction then undergoes protonolysis by a new terminal alkyne molecule, eliminating the (*E*)-**8** or (*E*)-**9** product (cycle B, step *iii*).

Under identical conditions, using *tert*-butylacetylene as the substrate, no Me_3Sn-functionalized enyne is observed, even after 12 h at 80 °C. However, after 3 days at 120 °C, the *tert*-butylacetylene is completely consumed, and ^1H, ^{13}C, and ^{119}Sn NMR spectroscopic analysis identifies the known $Me_3SnC{\equiv}C^tBu$[29] as the only Sn-containing species. The remainder of the *tert*-butylacetylene is converted to the known nonfunctionalized alkyne dimer via an established process.[14h,26]

Non-Pyridine Arenes as Substrates. To explore whether the aforementioned reactivity is unique to pyridine, a series of experiments was performed with a variety of heterocycle–$SnMe_3$ reagents. To facilitate observation of the various structures by NMR, cyclohexane-d_{12} was used as the solvent. A reaction under identical conditions using **1** and cyclohexylacetylene demonstrated that the choice of aromatic hydrocarbons or cyclohexane as solvent does not affect the reaction rate or products. When **1** and cyclohexylacetylene were added to catalyst **2b**, free pyridine was detected, indicating $-SnMe_3$ transfer. To evaluate whether a heterocycle is required in the Ar–$SnMe_3$ activation step, $PhSnMe_3$ was investigated as the substrate with cyclohexylacetylene. Additionally, both 2-(trimethylstannyl)thiophene and 2-(trimethylstannyl)furan were examined as $-SnMe_3$ sources. Importantly, negligible reaction of these Ar–$SnMe_3$ reagents is observed. However, within minutes at 25 °C, each of these mixtures results in complete alkyne conversion to the nonfunctionalized alkyne dimer,[14i] as determined by ^1H and ^{13}C NMR.

Disubstituted Alkynes and Alkenes as Substrates. Successful $-SnMe_3$ functionalization using terminal alkynes prompted exploration of other unsaturated substrates. To investigate the possibility of functionalizing internal alkynes, the reaction of **1** + 2-pentyne, catalyzed by **2b**, was investigated. However, under the reaction conditions used for terminal alkynes (60 °C, 12 h), there is no obvious catalytic turnover by

Scheme 7. Proposed Pathway for the Organolanthanide-Mediated Formation of Products (*E*)-8 and (*E*)-9 from Terminal Alkynes and 1

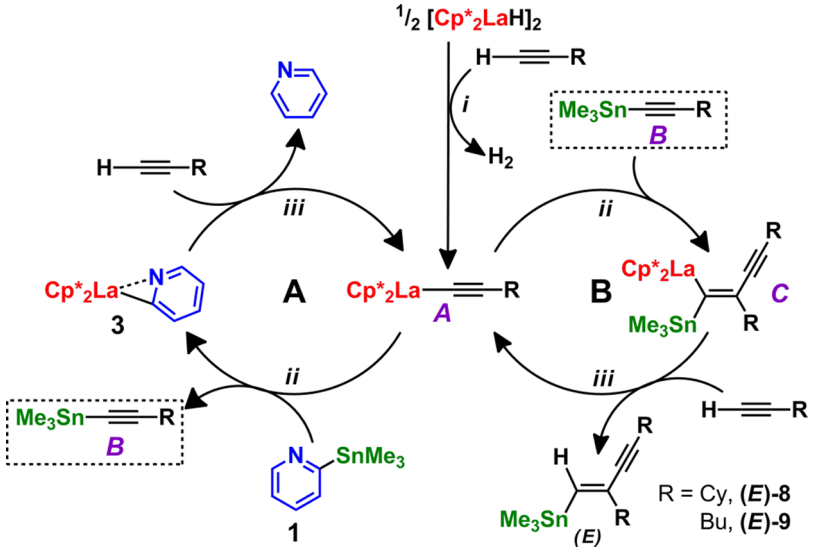

dx.doi.org/10.1021/om301031e | *Organometallics* XXXX, XXX, XXX–XXX

^{1}H NMR. The reaction temperature was then gradually increased, and after 2 days at 120 °C, there was still no obvious reaction. Additionally, a similar reaction was investigated using methylenecyclopentane as the substrate. Again, even after 2 days at 120 °C, no reaction was observable by ^{1}H NMR. These results indicate the chemistry described in Scheme 9 is only available to terminal alkynes.

DISCUSSION

Ethylene Insertion Reactivity. The reaction of **1** and ethylene, catalyzed by **2a**, is found to first yield compound **4** (Scheme 6). While activation of pyridine 2-C−SnR_3 groups by organolanthanide catalysts was previously unknown, it bears some similarity to the known activation of the pyridine 2-C−H position by organolanthanides, and it is plausible that the catalytic cycles follow similar pathways involving four-center transition states (Scheme 3).[14b,i] Importantly, the 2-C−$SnMe_3$ group reactivity is found to be significantly greater than that of the corresponding 2-C−H functionality. Reported mechanisms for lanthanide-mediated 2-C−H activation invoke pyridine precomplexation, followed by Ln−H/(pyridine)C−H σ-bond metathesis (Scheme 3),[14c,d,f,i,j] and such a pathway is plausible for C−Sn activation as well (Scheme 8). Indeed, the greater C−Sn bond length/steric accessibility relative to C−H (ca. 2.203 and 0.948 Å, respectively)[30] and weaker metalloid−C bond enthalpy[31] would appear to favor enhanced C−Sn reactivity. Furthermore, the greater C−$SnMe_3$ electron richness and length of the C−Sn bonds should promote agostic interactions with the electrophilic lanthanide metal ion, a likely prerequisite for C−Sn activation.[14c,d,f,i,j] While 2-(trimethylstannyl)pyridine (**1**) reacts readily with ethylene at 25 °C, 6-methyl-2-(trimethylstannyl)pyridine (**6**) fails to undergo detectable ethylene insertion. A plausible explanation is that the 6-methyl group of **6** significantly congests/destabilizes the four-center transition state (Scheme 8). The σ-bond metathesis step is likely severely hindered. This observation is in accord with related work on organoyttrium complexes, which readily metalate at the 2-hydrogen of pyridine but fail to metalate the corresponding 6-hydrogen of 2-picoline (Scheme 9).[17c] A similar explanation was invoked—the bulky substituent destabilizes the four-center transition state at the crowded Y center.

Scheme 8. Preferential C−Sn over C−H Bond Activation in 1, in the Context of the Reaction in Schemes 5 and 6[a]

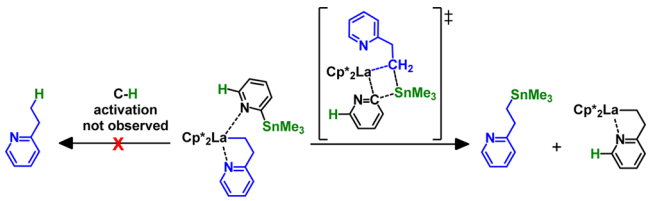

[a]For clarity, dative py→La interactions are not shown in the transition state.

Terminal Alkyne Reactivity. On the basis of the ethylene insertion chemistry described in Scheme 4, the initial expectation for terminal alkynyl substrates was a similar insertive process. However, terminal alkynes display reactivity distinctly different from that of ethylene in the reaction of **1** catalyzed by **2b**. For terminal alkynes, protonolytic reactivity greatly exceeds insertive reactivity (Scheme 10). This is reasonable, given that alkynyl protons are ~15 pK_a units more acidic than vinyl protons,[32] and the formation of the strong Cp*$_2$La−alkynyl bond (eq 5), ~93 kcal/mol[33] versus ~65 kcal/mol estimated for Cp*$_2$La(η^2-pyridyl) bonding,[34] represents a significant thermodynamic driving force. This reaction selectivity leads to the unexpected Sn-functionalized enyne products. The estimated reaction enthalpies (ΔH = $\sum\Delta H_{\text{bonds broken}} - \sum\Delta H_{\text{bonds formed}}$) for Cp*$_2$La−alkynyl and Cp*$_2$La($\eta^2$-pyridyl) were estimated as shown in Table 2.

Scheme 9. α-Methyl Group Deactivation of Pyridine Metalation in 6-Methyl-2-(trimethylstannyl)pyridine and α-Picoline with Organolanthanide and Organoyttrium Complexes[17c]

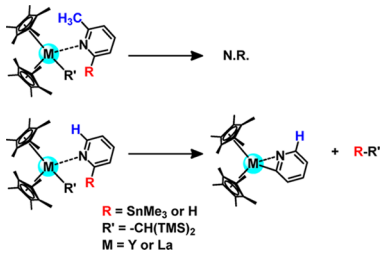

Scheme 10. Preferential Protonolysis by Alkyne versus Insertion into La−Pyridyl Species

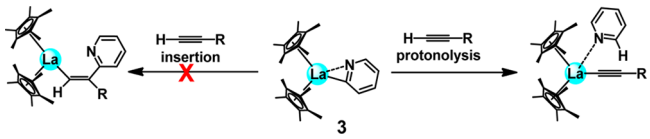

Table 2. Calculated Reaction Enthalpies for Cp*$_2$La−Alkynyl and Cp*$_2$La(η^2-pyridyl) Formation

Ln-H + H−≡−Me → Ln−≡−Me + H_2 (5)

Bonds Breaking	*Bond Dissociation Enthalpy*	*References*
Ln-H	54.2 kcal/mol	Ref. 32
H−≡−Ph	133.3 kcal/mol	Ref. 30b
Bonds Forming		
Ln−≡−Ph	93.2 kcal/mol[a]	Refs. 32, 34, and 36
H_2	104 kcal/mol	Ref. 30b
ΔH = (54.2 + 133.3) − (93.2 + 104.2) ≅ -9.9 kcal/mol		

Ln-H + Ar-$SnMe_3$ → Ln-Ar + H-$SnMe_3$ (6)

Bonds Breaking	*Bond Dissociation Enthalpy*	*References*
Ln-H	54.2 kcal/mol	Ref. 32
Ar-$SnMe_3$	85.6 kcal/mol	Ref. 30b
Bonds Forming		
Ln-Ar	56.4 kcal/mol[a]	Refs. 32, 34, and 35
Ln←heterocycle	7.8 kcal/mol	Ref. 32
H-$SnMe_3$	77.0 kcal/mol	Ref. 30b
ΔH = (54.2 + 85.6) − (56.4 + 7.8 + 77.0) ≅ -1.2 kcal/mol		

[a]With Ln/An adjustments.

These thermodynamic estimates agree with the experimental observations; specifically, the exothermic Ln−H + alkyne

dx.doi.org/10.1021/om301031e | Organometallics XXXX, XXX, XXX−XXX

reaction gives rise to La−alkynyl species and H_2, both detected by NMR spectroscopy. In contrast, the products of the essentially thermoneutral Ln−H + Sn−Ar reaction, in presence of alkynes, are not observed in the activation process by NMR spectroscopy. In previous organolanthanide-mediated alkyne dimerization studies, the Lewis base free reaction proceeds via $Cp^*_2Ln(\mu\text{-}C{\equiv}CR)_2LnCp^*_2$ dimers (eq 7).[38] In contrast,

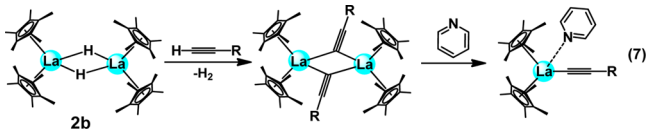

monomeric $Cp^*_2Ln(C{\equiv}CR)$(base) adducts suppress this pathway. Thus, the lack of nonstannylated alkyne dimerization activity in the present system suggests that pyridine (or **1** at the onset of reaction) acts to inhibit lanthanide−alkynyl dimer formation.

Initial observations on the final products of the **2b**-catalyzed cyclohexylacetylene + **1** reaction indicate that both (***E***)-**8** and (***Z***)-**8** product isomers are formed, as well as pyridine. A plausible catalytic cycle for the (***Z***)-**8** synthesis is shown in Scheme 11. Here species ***A***, the Cp^*_2Ln−alkynyl compound,

Scheme 11. One Possible Scenario for (*Z*)-8 Synthesis Mediated by an Organolanthanide Catalyst

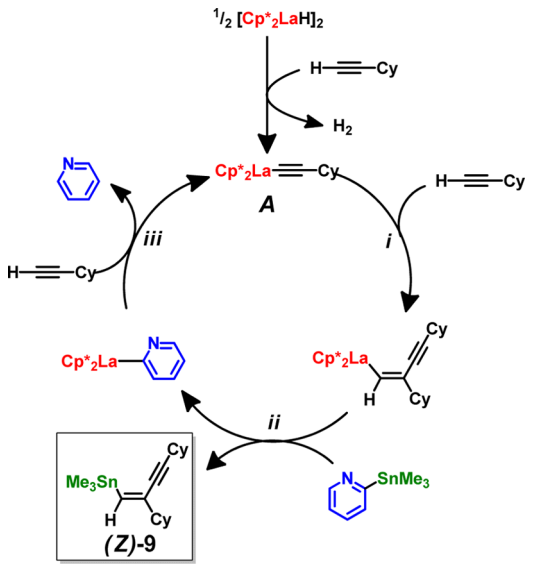

undergoes insertion by a second cyclohexylacetylene molecule (step *i*). Subsequent σ-bond metathesis (step *ii*) and protonolysis (step *iii*) release the Me_3Sn−enyne product. This scenario requires that free pyridine be produced concurrently with the Me_3Sn−enyne product. However, in situ NMR monitoring reveals that pyridine is produced quantitatively within minutes, before either (***E***)-**8** or (***Z***)-**8** is observed (see Figure 3), suggesting that Scheme 11 is not a significant contributor to the present catalytic process.

Scheme 7 invokes two distinct cycles, emphasizing that cycle A may operate independently of cycle B. The initiation of cycle B necessarily relies on Me_3Sn(alkynyl) species ***B*** produced by cycle A. The cycle begins with the thermodynamically favorable formation of Cp^*_2Ln−alkynyl species ***A*** from the precatalyst **2b**, a process known to proceed rapidly at 25 °C.[17c] In the present system, ***A*** initially undergoes carbostannolysis by **1** (step *ii*, cycle A, Scheme 7), yielding intermediate ***B*** and complex **2b**. In the next step (step *iii*, cycle A), **2b** undergoes protonolysis by terminal alkyne, regenerating ***A*** and releasing pyridine. The process in cycle A must transfer the Me_3Sn group of **1** to form complex ***B*** before cycle B is activated.

In cycle B (Scheme 7), complex ***B*** undergoes insertion into Cp^*_2La−alkynyl species ***A***, generating an intermediate Cp^*_2La−vinyl complex ***C***, which readily undergoes protonolysis by terminal alkyne, releasing the desired Me_3Sn-functionalized enyne, (***E***)-**8** or (***E***)-**9** (step *iii*, cycle B, Scheme 7). Complex ***A*** could potentially undergo terminal alkyne insertion rather than that of the Sn-substituted alkyne required in step *ii*, cycle B, Scheme 7. Indeed, in the absence of a Lewis base, f-element and group 3 metallocenes are reported to catalyze rapid (N_t > 5000 h^{-1} at 20 °C)[17c] protonolysis/insertion cycles, affording terminal alkyne dimers or oligomers.[17a,38b,39] However, the presence of a strong Lewis base such as pyridine significantly inhibits alkyne insertion.[14i,17c,40] In the present work, despite significant inhibition by Lewis basic pyridyl compounds, this insertion pathway is plausibly the source of small amounts of nonstannylated alkyne dimer formed as the more reactive organotin species are consumed.

Regarding competition between terminal alkynes and Me_3Sn-functionalized alkynes for insertion (step *ii*, cycle B, Scheme 7), it is demonstrated here that despite the increased Me_3Sn−group steric bulk, Me_3Sn-functionalized alkyne ***B*** preferentially undergoes insertion into ***A***. In related Cp^*_2La-mediated insertive processes, electron-rich TMS−alkynyl species are found to undergo insertion far more rapidly than terminal alkynes.[41] Similar trends are observed for Cp^*_2An-catalyzed (An = Th, U) alkyne insertion processes,[42] where the TMS substituent stabilizes the partial charges in the transition state −C≡C unit.[43] This preference likely reflects the known ability of group 14 substituents to stabilize β-positive charges—an effect which is enhanced for larger group 14 metals (see Figure 4).[44] Additional stabilization is doubtless imparted by favorable

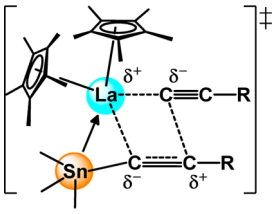

Figure 4. Potential stabilizing agostic interaction of an electron-rich −$SnMe_3$ substituent with electrophilic metal ion in the insertive transition state. For clarity, the arrow indicates a weak intermolecular stannane/organolanthanide interaction.

substituent−f-center agostic interactions (Figure 4),[45] and similar intermolecular stannane/organolanthanide interactions are supported by DFT analysis.[46]

The insertion of the Me_3Sn(alkynyl) species ***B*** explains the orientation of the initially formed product double bond. The data in Table 1 indicate that the kinetic product C=C orientation is predominantly *E*, and only subsequent heating yields appreciable quantities of the less hindered *Z* isomers, (***Z***)-**8** and (***Z***)-**9**. In addition to photoisomerization, vinylstannanes are known to undergo isomerization by thermally or chemically induced radical pathways.[13,27] In the present study, bond connectivity is established by HSQC and HMBC NMR, and double-bond orientation is assigned by NOESY NMR.

dx.doi.org/10.1021/om301031e | *Organometallics* XXXX, XXX, XXX−XXX

Observing (trimethylstannyl)alkynyl species ***B*** in the 25 °C reaction mixtures (Figure 5) provides support for the scenario

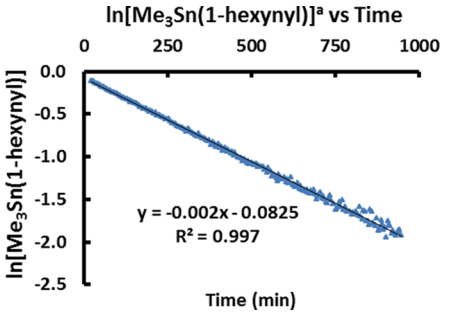

Figure 5. Plot of ln[Me_3Sn(1-hexynyl)] versus time, corresponding to cycle B, Scheme 7. (*a*) Due to overlapping signals in the ^1H NMR spectrum, the concentration of Me_3Sn(1-hexynyl) could not be integrated precisely and is determined by eq 8.

proposed in Scheme 7, which allows cycle A to proceed independently, generating free pyridine and intermediate ***B***. Indeed, for *tert*-butylacetylene, only cycle A is populated, while cycle B is not accessed. Presumably the observed product of cycle A, (trimethylstannyl)*tert*-butylethynyl, is too sterically encumbered for insertion at the Cp^*_2La- center, thereby impeding Me_3Sn-functionalized enyne formation via cycle B. As shown in Figure 5, the cycle A process (Scheme 7) is essentially complete by the initiation of kinetic monitoring. That is, **1** has reacted quantitatively with 1 equiv of free alkyne to yield 1 equiv of free pyridine and 1 equiv of species ***B***, the (trimethylstannyl)alkynyl intermediate, before cycle B is occupied. Therefore, the kinetic data only describe the processes of Scheme 7, cycle B. Species ***B*** is a reactant in cycle B; however, precise integration of the associated ^1H NMR signals is not possible due to signal overlap. For kinetic analysis, we assume that during cycle B, cycle A has already proceeded to quantitative completion and that depletion of species ***B*** corresponds to the simultaneous production of the Me_3Sn-functionalized enyne (**8** or **9**). For 1-hexyne as the substrate, the intermediate ***B*** concentration is described by eq 8. By estimating [***B***] in this manner, further kinetic analysis is then possible. Thus, plotting ln[***B***] versus time yields a linear plot, consistent with first-order rate dependence on [***B***] (Figure 5), corresponding to the proposed turnover-limiting insertive step *ii*, cycle B, of Scheme 7. Monitoring the Me_3Sn-functionalized intermediate and product concentrations over time at both the initial temperature of 25 °C and subsequent heating at 60 °C confirms the rapid formation of intermediate ***B*** and subsequent depletion at 60 °C (Figure 6).

$$[\boldsymbol{B}] = [\mathbf{1}]_0 - [\mathbf{8}] \quad (8)$$

Primary, secondary, and tertiary alkynes were also examined as substrates for catalytic Me_3Sn-functionalized enyne synthesis (Table 1). The general trend observed is that the less sterically hindered alkynes are more reactive, consistent with the steric demands of the insertive transition state (Figure 4)—a ubiquitous trend in organo-f-element alkyne insertion chemistry.[9d,17a,c,26b,38b,39,42,47] Note that the most encumbered substrate, *tert*-butylacetylene, completely resists insertion, even at elevated temperatures. That these rates are dominated by the alkyne substituent bulk is consistent with other data supporting the insertion step as turnover limiting.

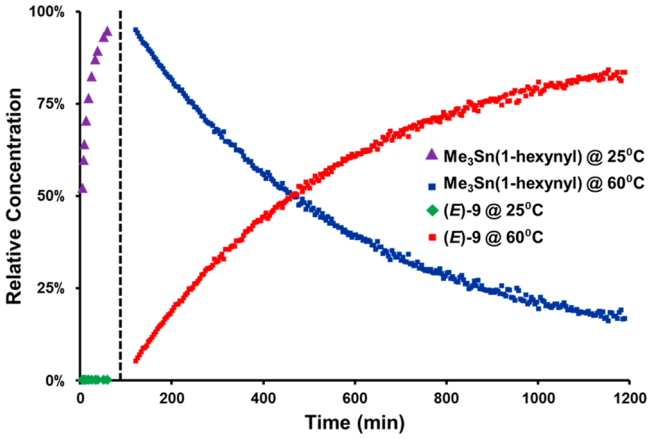

Figure 6. Relative concentrations of Me_3Sn intermediate ***B*** (Me_3Sn(1-hexynyl)) and product (***E***)-**9** during the reaction of **1** + 1-hexyne, catalyzed by **2b** (5 mol %): $[\mathbf{1}]_0$ = 294 mM; $[\text{1-hexyne}]_0$ = 706 mM; $[\mathbf{2b}]_0$ = 14.7 mM. At 60 °C, [***B***] is determined by eq 8. The dashed line indicates the change in reaction temperature from 25 to 60 °C.

Disubstituted Alkynes and Alkenes as Substrates. The successful activation of the heterocycle−$SnMe_3$ bond in **1** and subsequent ethylene insertion raises the question of whether other C−C unsaturated groups might exhibit similar reactivity. In previous work with Cp^*_2Y(2-pyridyl), it was reported that stoichiometric amounts of 2-pentyne react over the course of 2 days at 75 °C, producing a mixture of products that includes the 2,3- and 3,2-insertion products.[14i] However, in the present $[Cp^*_2LaH]_2$ system with excess **1**, no catalytic insertive reactivity with the internal alkyne is observed, even at 120 °C over 2 days. While H_2 is not observable by NMR in reactions with internal alkynes, Me_3SnH is observed as characteristic ^1H NMR spectral features at δ 4.65 ppm and a doublet at δ 0.13 ppm, suggesting C−$SnMe_3$ bond activation at the onset of reaction (eq 9).[48] Furthermore, the presence of a Lewis base

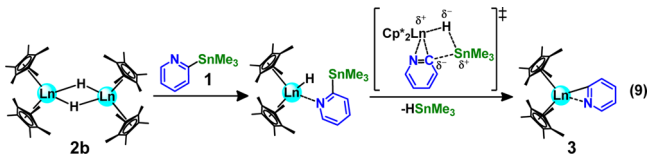

appears to inhibit cyclic disubstituted alkyne dimerization, known to be catalyzed by $Cp^*_2LaCH(SiMe_3)_2$.[47g] The lack of typical insertive reactivity in the present system is rationalized by considering the inhibitory effects of pyridine on lanthanocene insertion chemistry (vide supra).[14i] Under identical conditions, attempted reactions using methylenecyclopentane as the unsaturated substrate similarly failed to effect turnover. These observations, as well as the observation that even sterically slender terminal alkynes (e.g., 1-hexyne) do not undergo insertion at La-[2-(6-Me_3Sn)pyridyl] centers, argue that the high reactivity observed for terminal alkynes results from σ-bond metathesis involving the acidic terminal H−C≡C− moiety.

Effect of Varying Heterocycles. While regioselective pyridine C−H activation is generally challenging in other parts of the periodic table,[49] advances in this area have recently been reviewed by Nakao.[14b] However, compound **1** is known to undergo transmetalation exclusively at the 2-pyridyl−Sn bond in typical palladium-catalyzed Stille coupling processes.[50] In the present system, the reactivity of cyclohexylacetylene with Het−

dx.doi.org/10.1021/om301031e | *Organometallics* XXXX, XXX, XXX−XXX

$SnMe_3$ species (Het = non-pyridine heterocycle) stands in marked contrast to the results with **1**. Thus, when 2-(trimethylstannyl)thiophene, 2-(trimethylstannyl)furan, or trimethylphenyltin is used, rapid (<15 min) alkyne disappearance is observed by ^{1}H NMR at 25 °C, along with negligible Het−$SnMe_3$ reaction and only competing nonfunctionalized alkyne dimerization detectable. It appears that these heterocycles[15,20] are insufficiently strong Lewis bases to significantly inhibit rapid terminal alkyne dimerization mediated by Cp^*_2Ln- centers, which occurs at turnover frequencies greater than $\sim 10^3$ h^{-1} in the absence of strong Lewis bases.[14i] This suggests that the 2-pyridyl core has unique advantages as an organolanthanide-mediated Me_3Sn- delivery agent, with the pyridyl group serving a dual purpose in enabling this catalytic process: as an efficient Me_3Sn- delivery agent and as an inhibitor of competing alkyne dimerization.

CONCLUSIONS

The 2-(trimethylstannyl)pyridine C−Sn bond is found to be highly reactive with respect to Cp^*_2La-R activation (R = H, alkynyl), to catalytically deliver the Me_3Sn- group. While the Cp^*_2La-pyridyl product does not catalyze ethylene polymerization after the initial insertion, likely due to strong chelation in $Cp^*_2LaCH_2CH_2(2\text{-}NC_5H_4)$, a rich small-molecule chemistry has been discovered. Similar to the activation of *unfunctionalized* pyridine by other organolanthanide complexes, ethylene can be inserted at the 2-position. Insertion at the 2-$SnMe_3$ position of **1** is found to be strongly preferred over the 6-C−H position. In contrast to the reaction of unfunctionalized pyridine with terminal alkynes, the present system initiates a catalytic cycle using 2-(trimethylstannyl)pyridine which generates synthetically useful tin-functionalized enynes. Both α-monosubstituted and α-disubstituted alkynes are effective substrates, while α-trisubstituted alkynes appear to be too sterically encumbered to undergo efficient insertion. This work should provide a tool for accessing synthetically valuable tin-functionalized enynes and serve as a basis for potentially activating a broader range of heterocycle substituents with organo-f-element catalysts.

ASSOCIATED CONTENT

Supporting Information

Figures giving NMR and GC spectra of reaction products. This material is available free of charge via the Internet at http://pubs.acs.org.

AUTHOR INFORMATION

Corresponding Author

*E-mail: m-delferro@northwestern.edu (M.D.); t-marks@northwestern.edu (T.J.M.).

Author Contributions

The manuscript reflects the contributions of all authors. All authors have given approval to the final version of the manuscript.

Notes

The authors declare no competing financial interest.

ACKNOWLEDGMENTS

We thank the National Science Foundation (NSF, grants CHE-0809589 and CHE-1213235) for financial support. Use was made of the IMSERC facility at Northwestern University, supported by the National Science Foundation (NSF) under the grants CHE-1048773 (NMR) and CHE-0923236 (GC-TOF). We also thank Ms. E. Rabinovich for substrate synthesis.

REFERENCES

(1) (a) Lee, V. Y.; Sekiguchi, A. *Inorg. Chem.* **2011**, *50*, 12303−12314. (b) Miao, R.; Li, S.; Chiu, P. *Tetrahedron* **2007**, *63*, 6737−6740. (c) Espinet, P.; Echavarren, A. M. *Angew. Chem., Int. Ed.* **2004**, *43*, 4704−4734. (d) Orita, A.; Orita, J. Tin in Organic Synthesis. In *Main Group Metals in Organic Synthesis*; Yamamoto, H., Oshima, K., Eds.; Wiley-VCH: Weinheim, Germany, 2004; Vol. *2*, pp 621−708. (e) Alonso, F.; Beletskaya, I. P.; Yus, M. *Chem. Rev.* **2002**, *102*, 4009−4092. (f) Neumann, W. P. *J. Organomet. Chem.* **1992**, *437*, 23−39. (g) Mitchell, T. N. *Synthesis* **1992**, *9*, 803−815.

(2) (a) Ishihara, K. Sn(II) and Sn(IV) Lewis Acids. In *Lewis Acids in Organic Synthesis*; Wiley-VCH: Weinheim, Germany, 2008; pp 395−452. (b) Stille, J. K. *Pure Appl. Chem.* **1985**, *57*, 1771−1780. (c) Sheffy, F. K.; Godschalx, J. P.; Stille, J. K. *J. Am. Chem. Soc.* **1984**, *106* (17), 4833−4840.

(3) (a) Beaini, S.; Deacon, G. B.; Delbridge, E. E.; Junk, P. C.; Skelton, B. W.; White, A. H. *Eur. J. Inorg. Chem.* **2008**, 4586−4596. (b) Beaini, S.; Deacon, G. B.; Hilder, M.; Junk, P. C.; Turner, D. R. *Eur. J. Inorg. Chem.* **2006**, 3434−3441. (c) Cetinkaya, B.; Hitchcock, P. B.; Lappert, M. F.; Smith, R. G. *J. Chem. Soc., Chem. Commun.* **1992**, 932−934.

(4) (a) Deacon, G. B.; Junk, P. C.; Urbatsch, A. *Eur. J. Inorg. Chem.* **2011**, *2011*, 3592−3600. (b) Deacon, G. B.; Junk, P. C.; Moxey, G. J. *Chem. Asian J.* **2009**, *4*, 1717−1728. (c) Cole, M. L.; Deacon, G. B.; Forsyth, C. M.; Junk, P. C.; Konstas, K.; Wang, J. *Chem. Eur. J.* **2007**, *13*, 8092−8110.

(5) (a) Nakao, Y.; Satoh, J.; Shirakawa, E.; Hiyama, T. *Angew. Chem., Int. Ed.* **2006**, *45*, 2271−2274. (b) Shirakawa, E.; Nakayama, K.; Morita, R.; Tsuchimoto, T.; Kawakami, Y.; Matsubara, T. *Bull. Chem. Soc. Jpn.* **2006**, *79*, 1963−1976. (c) Shimizu, M.; Jiang, G.; Murai, M.; Takeda, Y.; Nakao, Y.; Hiyama, T.; Shirakawa, E. *Chem. Lett.* **2005**, *34*, 1700−1701. (d) Yoshida, H.; Honda, Y.; Shirakawa, E.; Hiyama, T. *Chem. Commun.* **2001**, 1880−1881. (e) Yoshida, H.; Shirakawa, E.; Nakao, Y.; Honda, Y.; Hiyama, T. *Bull. Chem. Soc. Jpn.* **2001**, *74*, 637−647. (f) Yoshida, H.; Shirakawa, E.; Kurahashi, T.; Nakao, Y.; Hiyama, T. *Organometallics* **2000**, *19*, 5671−5678. (g) Shirakawa, E.; Hiyama, T. *J. Organomet. Chem.* **1999**, *576*, 169−178. (h) Shirakawa, E.; Yamasaki, K.; Yoshida, H.; Hiyama, T. *J. Am. Chem. Soc.* **1999**, *121*, 10221−10222. (i) Shirakawa, E.; Yoshida, H.; Nakao, Y.; Hiyama, T. *J. Am. Chem. Soc.* **1999**, *121*, 4290−4291. (j) Shirakawa, E.; Yoshida, H.; Kurahashi, T.; Nakao, Y.; Hiyama, T. *J. Am. Chem. Soc.* **1998**, *120*, 2975−2976.

(6) Stille, J. K. *Angew. Chem.* **1986**, *98*, 504−519; *Angew. Chem., Int. Ed. Engl.* **1986**, 25, 508−523.

(7) (a) Kong, K.; Moussa, Z.; Lee, C.; Romo, D. *J. Am. Chem. Soc.* **2011**, *133*, 19844−19856. (b) Hamze, A.; Provot, O.; Brion, J.-D.; Alami, M. *J. Org. Chem.* **2007**, *72*, 3868−3874. (c) Guanti, G.; Riva, R. *Org. Biomol. Chem.* **2003**, *1*, 3967−3976.

(8) Fugami, K.; Kosugi, M., Organotin Compounds. In *Cross-Coupling Reactions*; Miyaura, N., Ed.; Springer: Berlin/Heidelberg, Germany, 2002; Vol. *219*, pp 87−130.

(9) (a) Chen, Z.; Huang, G.; Jiang, H.; Huang, H.; Pan, X. *J. Org. Chem.* **2011**, *76*, 1134−1139. (b) Zhang, X.; Lu, Z.; Fu, C.; Ma, S. *J. Org. Chem.* **2010**, *75*, 2589−2598. (c) Schneider, C. C.; Caldeira, H.; Gay, B. M.; Back, D. F.; Zeni, G. *Org. Lett.* **2010**, *12*, 936−939. (d) Seo, S. Y.; Yu, X. H.; Marks, T. J. *J. Am. Chem. Soc.* **2009**, *131*, 263−276. (e) Qing, F.-L.; Gao, W.-Z.; Ying, J. *J. Org. Chem.* **2000**, *65*, 2003−2006. (f) Gabriele, B.; Salerno, G.; Lauria, E. *J. Org. Chem.* **1999**, *64*, 7687−7692.

(10) Platel, R. H.; Schafer, L. L. *Chem. Commun.* **2012**, *48*, 10609−10611.

(11) Gielen, M. *Appl. Organomet. Chem.* **2002**, *16*, 481−494.

(12) Shi, Y.; Peterson, S. M.; Haberaecker, W. W.; Blum, S. A. *J. Am. Chem. Soc.* **2008**, *130*, 2168−2169.

(13) Miura, K.; Saito, H.; Itoh, D.; Matsuda, T.; Fujisawa, N.; Wang, D.; Hosomi, A. *J. Org. Chem.* **2001**, *66*, 3348−3355.

(14) (a) Guan, B.-T.; Hou, Z. *J. Am. Chem. Soc.* **2011**, *133*, 18086−18089. (b) Nakao, Y. *Synthesis* **2011**, *20*, 3209−3219. (c) Kramer, M. U.; Yahia, A.; Maron, L.; Okuda, J. *C. R. Chim.* **2010**, *13*, 626−632. (d) Yahia, A.; Kramer, M. U.; Okuda, J.; Maron, L. *J. Organomet. Chem.* **2010**, *695*, 2789−2793. (e) Carver, C. T.; Diaconescu, P. L. *J. Am. Chem. Soc.* **2008**, *130*, 7558−7559. (f) Jantunen, K. C.; Scott, B. L.; Gordon, J. C.; Kiplinger, J. L. *Organometallics* **2007**, *26*, 2777−2781. (g) Arndt, S.; Elvidge, B. R.; Zeimentz, P. M.; Spaniol, T. P.; Okuda, J. *Organometallics* **2005**, *25*, 793−795. (h) Duchateau, R.; Brussee, E. A. C.; Meetsma, A.; Teuben, J. H. *Organometallics* **1997**, *16*, 5506−5516. (i) Deelman, B.-J.; Stevels, W. M.; Teuben, J. H.; Lakin, M. T.; Spek, A. L. *Organometallics* **1994**, *13*, 3881−3891. (j) Thompson, M. E.; Baxter, S. M.; Bulls, A. R.; Burger, B. J.; Nolan, M. C.; Santarsiero, B. D.; Schaefer, W. P.; Bercaw, J. E. *J. Am. Chem. Soc.* **1987**, *109* (1), 203−219. (k) Watson, P. L. *J. Chem. Soc., Chem. Commun.* **1983**, 276−277. (l) Kaneko, H.; Nagae, H.; Tsurugi, H.; Mashima, K. *J. Am. Chem. Soc.* **2011**, *133*, 19626−19629.

(15) Ringelberg, S. N.; Meetsma, A.; Troyanov, S. I.; Hessen, B.; Teuben, J. H. *Organometallics* **2002**, *21*, 1759−1765.

(16) Ringelberg, S. N.; Meetsma, A.; Hessen, B.; Teuben, J. H. *J. Am. Chem. Soc.* **1999**, *121*, 6082−6083.

(17) (a) Duchateau, R.; van Wee, C. T.; Meetsma, A.; Teuben, J. H. *J. Am. Chem. Soc.* **1993**, *115*, 4931−4932. (b) Booij, M.; Deelman, B. J.; Duchateau, R.; Postma, D. S.; Meetsma, A.; Teuben, J. H. *Organometallics* **1993**, *12*, 3531−3540. (c) Den Haan, K. H.; Wielstra, Y.; Teuben, J. H. *Organometallics* **1987**, *6*, 2053−2060.

(18) Luo, G.; Luo, Y.; Qu, J.; Hou, Z. *Organometallics* **2012**, *31*, 3930−3937.

(19) Jordan, R. F.; Taylor, D. F. *J. Am. Chem. Soc.* **1989**, *111*, 778−779.

(20) Hessen, B.; Ringelberg, S. N.; Meppelder, G.-J.; Teuben, J. H. *Polym. Prepr.* **2000**, *41*, 397−398.

(21) Jeske, G.; Lauke, H.; Mauermann, H.; Swepston, P. N.; Schumann, H.; Marks, T. J. *J. Am. Chem. Soc.* **1985**, *107*, 8091−8103.

(22) Sasabe, M.; Houda, Y.; Takagi, H.; Sugane, T.; Bo, X.; Yamamura, K. *J. Chem. Soc., Perkin Trans. 1* **2000**, 3786−3790.

(23) Rossi, R.; Carpita, A.; Ciofalo, M.; Lippolis, V. *Tetrahedron* **1991**, *47*, 8443−8460.

(24) Bianchini, C.; Gatteschi, D.; Giambastiani, G.; Guerrero Rios, I.; Ienco, A.; Laschi, F.; Mealli, C.; Meli, A.; Sorace, L.; Toti, A.; Vizza, F. *Organometallics* **2007**, *26*, 726−739.

(25) (a) Ansyln, E. V.; Dougherty, D. A. *Modern Physical Organic Chemistry*; University Science Books: Sausalito, CA, 2006. (b) Espenson, J. H. *Chemical Kinetics and Reaction Mechanisms*, 2nd ed.; McGraw-Hill: New York, 1995. (c) Pilling, M. J.; Seakins, P. W. *Reaction Kinetics*; Oxford University Press: New York, 1995.

(26) (a) Komeyama, K.; Kawabata, T.; Takehira, K.; Takaki, K. *J. Org. Chem.* **2005**, *70*, 7260−7266. (b) Heeres, H. J.; Teuben, J. H. *Organometallics* **1991**, *10*, 1980−1986.

(27) (a) ter Wiel, M. K. J.; Kwit, M. G.; Meetsma, A.; Feringa, B. L. *Org. Biomol. Chem.* **2007**, *5*, 87−96. (b) Kelly, J. M. *J. Chem. Soc., Dalton Trans.* **1984**, 909−914. (c) Vanderlinden, P.; Boue, S. *J. Organomet. Chem.* **1975**, *87*, 183−188. (d) Seyferth, D.; G. Vaughan, L. *J. Organomet. Chem.* **1963**, *1*, 138−152.

(28) Wrackmeyer, B. *J. Organomet. Chem.* **1978**, *145*, 183−188.

(29) (a) Mitchell, T. N. *J. Organomet. Chem.* **1977**, *141*, 289−293. (b) Seyferth, D.; White, D. L. *J. Organomet. Chem.* **1971**, *32*, 317−322.

(30) The average distances found in the Cambridge Crystallographic Data centre (CDC, Oct. 2012) for pyridyl groups with 2-Sn and 6-H substitution: C−Sn = 2.203 Å and C−H = 0.948 Å.

(31) (a) Blanksby, S. J.; Ellison, G. B. *Acc. Chem. Res.* **2003**, *36*, 255−263. (b) Davies, A. G., In *Tin Chemistry: Fundamentals, Frontiers, and Applications*; Davies, A. G., Gielen, M., Pannell, K. H., Tiekink, R. T., Eds.; Wiley: Chichester, U.K., 2008; pp 1−14.

(32) Bordwell, F. G. *Acc. Chem. Res.* **1988**, *21*, 456−463.

(33) Nolan, S. P.; Stern, D.; Marks, T. J. *J. Am. Chem. Soc.* **1989**, *111*, 7844−7853.

(34) Estimated from the sum of Ln−phenyl and Ln−thf coordination bond disruption enthalpies. See ref 30.

(35) Bruno, J. W.; Stecher, H. A.; Morss, L. R.; Sonnenberger, D. C.; Marks, T. J. *J. Am. Chem. Soc.* **1986**, *108*, 7275−7280.

(36) Nolan, S. P.; Porchia, M.; Marks, T. J. *Organometallics* **1991**, *10*, 1450−1457.

(37) Schock, L. E.; Seyam, A. M.; Sabat, M.; Marks, T. J. *Polyhedron* **1988**, *7*, 1517−1529.

(38) (a) Forsyth, C. M.; Nolan, S. P.; Stern, C. L.; Marks, T. J.; Rheingold, A. L. *Organometallics* **1993**, *12*, 3618−3623. (b) Evans, W. J.; Keyer, R. A.; Ziller, J. W. *Organometallics* **1993**, *12*, 2618−2633.

(39) (a) Straub, T.; Haskel, A.; Eisen, M. S. *J. Am. Chem. Soc.* **1995**, *117*, 6364−6365. (b) Heeres, H. J.; Nijhoff, J.; Teuben, J. H.; Rogers, R. D. *Organometallics* **1993**, *12*, 2609−2617.

(40) (a) Haskel, A.; Wang, J. Q.; Straub, T.; Neyroud, T. G.; Eisen, M. S. *J. Am. Chem. Soc.* **1999**, *121*, 3025−3034. (b) Li, Y.; Marks, T. J. *J. Am. Chem. Soc.* **1998**, *120*, 1757−1771. (c) St. Clair, M.; Schaefer, W. P.; Bercaw, J. E. *Organometallics* **1991**, *10*, 525−527.

(41) (a) Hong, S.; Marks, T. J. *Acc. Chem. Res.* **2004**, *37*, 673−686. (b) Li, Y.; Marks, T. J. *J. Am. Chem. Soc.* **1996**, *118*, 9295−9306. (c) Li, Y. W.; Fu, P. F.; Marks, T. J. *Organometallics* **1994**, *13*, 439−440.

(42) (a) Stubbert, B. D.; Marks, T. J. *J. Am. Chem. Soc.* **2007**, *129*, 6149−6167. (b) Stubbert, B. D.; Marks, T. J. *J. Am. Chem. Soc.* **2007**, *129* (14), 4253−4271.

(43) (a) Brinkman, E. A.; Berger, S.; Brauman, J. I. *J. Am. Chem. Soc.* **1994**, *116*, 8304−8310. (b) Hopkinson, A. C.; Lien, M. H. *J. Org. Chem.* **1981**, *46*, 998−1003.

(44) (a) Nguyen, K. A.; Gordon, M. S.; Wang, G. T.; Lambert, J. B. *Organometallics* **1991**, *10*, 2798−2803. (b) Lambert, J. B.; Wang, G. T.; Teramura, D. H. *J. Org. Chem.* **1988**, *53*, 5422−5428.

(45) (a) Seo, S.; Yu, X.; Marks, T. J. *J. Am. Chem. Soc.* **2008**, *131*, 263−276. (b) Schumann, H.; Meese-Marktscheffel, J. A.; Esser, L. *Chem. Rev.* **1995**, *95*, 865−986. (c) Koga, N.; Morokuma, K. *J. Am. Chem. Soc.* **1988**, *110*, 108−112.

(46) Raynaud, C.; Perrin, L.; Maron, L. *Organometallics* **2006**, *25*, 3143−3151.

(47) (a) Weiss, C. J.; Marks, T. J. *Dalton Trans.* **2010**, *39*, 6576−6588. (b) Weiss, C. J.; Wobser, S. D.; Marks, T. J. *Organometallics* **2010**, *29*, 6308−6320. (c) Seo, S.; Marks, T. J. *Chem. Eur. J.* **2010**, *16*, 5148−5162. (d) Weiss, C. J.; Wobser, S. D.; Marks, T. J. *J. Am. Chem. Soc.* **2009**, *131*, 2062−2063. (e) Yu, X. H.; Seo, S.; Marks, T. J. *J. Am. Chem. Soc.* **2007**, *129*, 7244−7245. (f) Li, Y.; Marks, T. J. *J. Am. Chem. Soc.* **1996**, *118*, 707−708. (g) Heeres, H. J.; Heeres, A.; Teuben, J. H. *Organometallics* **1990**, *9*, 1508−1510.

(48) Zhou, D.; Reiche, C.; Nag, M.; Soderquist, J. A.; Gaspar, P. P. *Organometallics* **2009**, *28*, 2595−2608.

(49) Wen, P.; Li, Y.; Zhou, K.; Ma, C.; Lan, X.; Ma, C.; Huang, G. *Adv. Synth. Catal.* **2012**, *354*, 2135−2140.

(50) (a) Blanck, S.; Maksimoska, J.; Baumeister, J.; Harms, K.; Marmorstein, R.; Meggers, E. *Angew. Chem., Int. Ed.* **2012**, *51*, 5244−5246. (b) Blanck, S.; Cruchter, T.; Vultur, A.; Riedel, R.; Harms, K.; Herlyn, M.; Meggers, E. *Organometallics* **2011**, *30*, 4598−4606. (c) Schwab, P. F. H.; Fleischer, F.; Michl, J. *J. Org. Chem.* **2002**, *67*, 443−449.